



Oxovanadium catalyst based on nano-porous carbon xerogel: an efficient heterogeneous nano-catalyst for aerobic oxidation of olefins

Tahereh Mokary Yazdely, Massomeh Ghorbanloo*, Hassan Hosseini-Monfared

Department of Chemistry, Faculty of Science, University of Zanjan, 45371-38791 Zanjan, Iran, Tel. +98-24-33054084; Fax: +98-24-33052477; emails: m_ghorbanloo@yahoo.com (M. Ghorbanloo), t.Mokari85@gmail.com (T.M. Yazdely), monfared@znu.ac.ir (H.H. Monfared)

Received 20 September 2018; Accepted 3 April 2019

ABSTRACT

Porous carbon xerogels were prepared from the sol-gel polymerization of resorcinol with formaldehyde (RF) followed by carbonization at a high temperature under argon atmosphere. The capacity of the carbon xerogels for direct immobilization of metal complexes was tested with a vanadium(IV) complex, $[V^{IV}O(HL)(H_2O)(CH_3OH)]$, which possesses an extended ligand π system and reactive hydroxyl groups on the *L*-tyrosine fragment. Textural characterization of the CXG and CXG/ $[V^{IV}O(HL)(H_2O)(CH_3OH)]$ have been investigated using N_2 adsorption–desorption at $-196^\circ C$. Chemical surface groups were analyzed by FT-IR spectroscopy. Nano-particle size and morphology of CXG and CXG/ $[V^{IV}O(HL)(H_2O)(CH_3OH)]$ nano-particles have been characterized by scanning electron microscopy (SEM). Catalytic activity of CXG/ $[VO(HL)(H_2O)(CH_3OH)]$ was investigated in the aerobic oxidation of olefins. The reaction conditions have been optimized for solvent and temperature. CXG/ $[VO(HL)(H_2O)(CH_3OH)]$ showed higher catalytic activity for the epoxidation of unfunctionalized olefins with molecular oxygen in the presence of isobutyraldehyde. Comparison of the heterogenized catalyst, CXG/ $[VO(HL)(H_2O)(CH_3OH)]$, with the corresponding homogeneous catalyst, $[VO(HL)(H_2O)(CH_3OH)]$, showed that the heterogeneous catalyst had higher activity and selectivity than the homogeneous counterpart. The heterogeneous catalyst was easily recovered from the reaction medium and could be re-used for other five runs without significant loss of activity.

Keywords: Xerogel; Aerobic oxidation; Oxovanadium; Nano-porous; Nano-particles

1. Introduction

Carbon gels such as xerogels, aerogels, and cryogels are classified as nanostructure carbons, as their structure and texture can be designated and controlled at nanometer scale [1]. Carbon gels are synthesized by carbonization of organic gels, which are prepared by the sol-gel polycondensation of organic monomers, such as resorcinol and formaldehyde, by using Pekala's method [2].

Carbon xerogels have received noteworthy attention in the literature over the past decade and can be produced in

different forms (as powder, thin-film, cylinders, spheres, discs, or can be custom shaped) [3]. The most important properties of these materials are their high porosity, surface area and pore volume, controllable pore structure, narrow and controlled pore size distribution, low electrical resistivity and outstanding thermal and mechanical properties. Due to these advantageous, carbon xerogel based materials are attractive candidates in a wide range of applications such as electrode material for double layer capacitors or supercapacitors [4–6], adsorption materials for gas separation [7], column packing materials for chromatography [8], for H_2 storage [9] and catalyst supports [10–13].

* Corresponding author.

The performance of carbon materials in catalysis depends on their surface properties. The surface chemistry of the carbon material plays a most important role on its catalytic properties, providing active sites capable of chemisorbing the reactants and forming surface intermediates of sufficient strength. Oxygen groups can be introduced on the surface of carbon xerogels by treatment with a variety of oxidizing agents, in the gas and liquid phases [14]. Liquid phase oxidation can be performed in a Soxhlet with nitric acid under reflux [15]. Large amounts of carboxylic groups are introduced, together with phenol and carbonyl groups. Carboxylic acids can react with molecules containing $-OH$ or $-NH_2$ functions provides for ester or amide linkages, respectively. This approach was used to anchor Schiff base Ni complexes with amine groups onto an activated carbon oxidized with HNO_3 [16]. In the case of carbonyl surface groups, nucleophilic attack from the hydroxyl group originates an ether bond; in the case of carboxylic anhydride groups, an ester bond and a surface carboxylic acid group are formed.

We have been exploiting the surface properties of activated carbons for the immobilization of vanadium complex with Schiff base type ligands. Similar methodologies were used by Román Martínez et al. [17] to anchor a Rh complex [17] and Mahata et al. [18] to anchor a manganese(III) salen complex [18] onto an activated carbon support. The activated carbons with immobilized metal complexes with catalytic properties were found to be efficient and re-usable in various catalytic reactions [19–21]. However, in general, the slow diffusion of reactants through the micropores or mesopores of activated carbon supports makes the heterogenized catalysts less active than the corresponding homogeneous catalysts. This limitation can be overcome by using surface of carbon materials as supports for metal complexes, as diffusion of the reactant and product molecules are expected to be much easier.

Herein we are reporting on a development of a heterogenized carbon xerogel based catalyst through the anchoring of oxovanadium complex onto the activated carbon xerogels surface with effective catalytic properties for oxidation reactions. Covalent bonding of the complex onto the activated carbon surface prevents leaching, leading to stable and reusable catalysts.

As a result, the anchored complexes were found to be very stable and reusable catalysts for the catalytic activity [18]. Similar examples for [Metal(salen)], Cu(II) complex with salen ligands, Mn(III) salen complexes, chiral Mn(III) salen complex (Jacobsen catalyst), etc, are discussed in various literatures [18,22,23].

2. Experimental

2.1. Materials and equipment

Materials resorcinol (Merck 99%, Germany), formaldehyde (Merck 37%, Germany), sodium hydroxide (Merck 99%, Germany), *L*-tyrosine (Merck 98%, Germany), salicylaldehyde (Merck 99%, Germany), $VO(acac)_2$ (Merck 98%, Germany) were used in $CXG/[VO(HL)(H_2O)(CH_3OH)]$ preparation. All chemicals were used as received without further purification. FT-IR spectra were recorded in KBr disks with a Bruker FT-IR spectrophotometer, USA. Oxidation state of vanadium has been determined by cyclic voltmeter (SAMA500 potentiostat electrochemical analyzer). The exact amount of the vanadium in the compounds was determined by AA, Varian 110. Elemental analyses were determined on a PerkinElmer CHN 2400 analyzer. The separation of heterogeneous catalyst from reaction media was assisted by a high speed centrifuge (Sigma-Aldrich, USA, 3–30 K). Morphology of compounds was investigated with SEM via MIRA3 FEG SEM (Tescan, Czech Republic) and an accelerating voltage of 10 keV. XRD patterns were recorded on a Bruker D8ADVANCE (USA), X-ray diffractometer with Cu K_α target ($k = 1.54 \text{ \AA}$). N_2 sorption analysis was performed at 77 K using a PHS-1020 (PHSCHINA) equipped with an automated surface area and pore size analyzer. Before analysis, samples were degassed at $130^\circ C$ or $150^\circ C$ for 20 h using a “Masterprep” degassing system. BET surface areas were determined over a P/P_0 range. The reaction products of oxidation were determined and analyzed using an HP Agilent 6890 gas chromatograph equipped with a HP-5 capillary column (phenyl methyl siloxane $30 \text{ m} \times 320 \mu\text{m} \times 0.25 \mu\text{m}$).

2.2. Synthesis of oxovanadium complex $[VO(HL)(H_2O)(CH_3OH)]$

The Schiff base ligand H_3L was synthesized by the condensation of salicylaldehyde with *L*-tyrosine in 1:1 molar ratio in methanol [24,25]. Its vanadium complex was prepared with high yield from the reaction of H_3L with an equimolar amount of $VO(acac)_2$ in MeOH, as shown in Fig. 1. The complex was obtained as a dark green powder. The elemental analysis corresponds to the general formula $[V^{IV}O(HL)(H_2O)(CH_3OH)]$, which was further confirmed by atomic absorption spectroscopy analysis and cyclic voltammeter. CHN analysis: Calc.: C 51.01%, H 4.78%, N 3.50%, V 12.73%. Found: C 49.88%, H 4.91%, N 3.47%, V 12.68%.

Selected FT-IR (KBr, cm^{-1}) H_3L : 3,211 (w); 3,026 (w); 2,976 (w); 2,919 (w); 1,612 (vs); 1,596 (s); 1,531 (m); 1,457 (m); 1,397 (m); 1,366 (m); 1,332 (s); 1,247 (s); 1,102 (m); 1,045 (m); 843 (s); 741 (m); 653 (s); 576 (s); 493 (w).

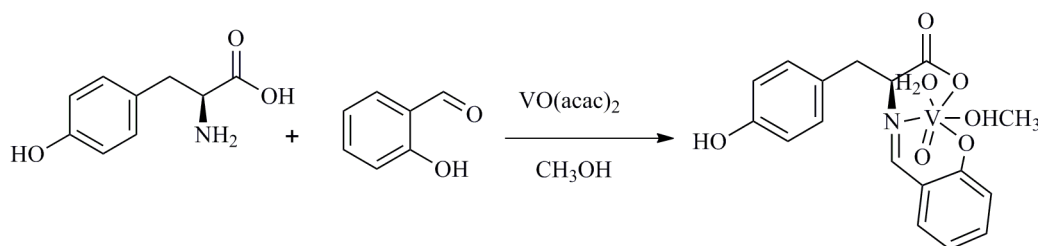


Fig. 1. Schematic synthesis of oxovanadium complex $[V^{IV}O(HL)(H_2O)(CH_3OH)]$.

Selected FT-IR (KBr, cm^{-1}) $[\text{V}^{\text{IV}}\text{O}(\text{HL})(\text{H}_2\text{O})(\text{CH}_3\text{OH})]$: 3,464 (br); 2,942 (w); 2,875 (w); 1,640 (s); 1,520 (s); 1,452 (s); 1,396 (m); 1,276 (w); 1,157 (w); 1,032 (w); 948 (s); 833 (w); 768 (w); 670 (w); 542 (w).

2.3. Synthesis of organogel (OG)

Organogel was obtained from the sol-gel polymerization of resorcinol (R) and formaldehyde (F) in methanol. Sodium hydroxide was utilized as catalyst (C). All gels were synthesized using the stoichiometric R/F molar ratio (1:2), 20 as the R/C molar ratio and 3.93 as the dilution molar ratio (i.e., methanol/R + F + C). For this purpose, 0.0072 g of sodium hydroxide was dissolved in 53 mL of methanol, 15.96 g of resorcinol were added with continuous stirring. Finally, 22 mL of formaldehyde were added under stirring. After the dissolution of sodium hydroxide and resorcinol in methanol, formaldehyde was added under stirring. Then the pH was adjusted to 7.0 by addition of diluted HNO_3 . Stirring was continued for 30 min, after which the mixture was poured into cylindrical glass tubes [26]. These tubes were sealed and introduced into a water bath at 50°C . Samples were then dried in an autoclave at 150°C for 5 h.

Selected FT-IR (KBr, cm^{-1}): 3,464 (br, s); 2,942 (w); 2,874 (w); 2,367 (w); 1,622 (vs); 1,479 (s); 1,385 (s); 1,314 (w); 1,228 (w); 1,207 (w); 1,094 (s); 849 (w); 805 (w); 669 (w).

2.4. Synthesis of carbon xerogel

Carbon xerogel was obtained by pyrolyzing dried gels under argon flow ($100 \text{ cm}^3 \text{ min}^{-1}$) at 800°C in a tubular furnace. The heating program included the following sequential steps in flowing argon: (1) ramp at 2°C min^{-1} to 400°C and hold for 60 min; (2) ramp at 2°C min^{-1} to 600°C and hold for 60 min; (3) ramp at 2°C min^{-1} to 800°C and hold for 360 min; (4) cool slowly to room temperature [18].

Selected FT-IR (KBr, cm^{-1}): 3,458 (br, s); 2,927 (w); 2,858 (w); 1,657 (m); 1,590 (w); 1,473 (w); 1,094 (s); 829 (w).

2.5. Activation of carbon xerogel surface

Carbon xerogel surface was activated in a Soxhlet with nitric acid (5 M) under reflux and nitrogen atmosphere for 48 h [27]. The oxidized materials were subsequently washed with distilled water until neutral pH, and dried in an oven at 110°C for 24 h.

Selected FT-IR (KBr, cm^{-1}) activated carbogel: 3,446 (br, s); 2,929 (m); 2,860 (w); 2,151 (w); 1,922 (w); 1,733 (s); 1,590 (s); 1,154 (vs).

2.6. Anchoring of the oxovanadium complex on CXG surface ($\text{CXG}/[\text{V}^{\text{IV}}\text{O}(\text{HL})(\text{H}_2\text{O})(\text{CH}_3\text{OH})]$)

The $[\text{V}^{\text{IV}}\text{O}(\text{HL})(\text{H}_2\text{O})(\text{CH}_3\text{OH})]$ complex was directly immobilized onto the supports by refluxing for 48 h 1 g of carbon xerogel with 74 mg (185 μmol) of $[\text{V}^{\text{IV}}\text{O}(\text{HL})(\text{H}_2\text{O})(\text{CH}_3\text{OH})]$ in 150 mL methanol under nitrogen atmosphere, as shown in Fig. 2. The resulting materials were washed several times with methanol, in order to remove any physically adsorbed complex [28], and finally the materials were dried at 60°C .

Selected FT-IR (KBr, cm^{-1}) xerogel/ $[\text{V}^{\text{IV}}\text{O}(\text{HL})(\text{H}_2\text{O})(\text{CH}_3\text{OH})]$: 3,464 (br); 2,940 (w); 2,874 (w); 1,728 (s); 1,597 (s); 1,489 (w); 1,251 (s); 1,182 (w); 1,116 (br); 934 (w); 844 (w); 669 (m).

2.7. General oxidation procedures

A mixture of $\text{CXG}/[\text{V}^{\text{IV}}\text{O}(\text{HL})(\text{H}_2\text{O})(\text{CH}_3\text{OH})]$ (0.0850 $\mu\text{mol V}^{\text{IV}}$) in CH_3CN (5.00 mL) was placed into a two-necked flask equipped with a magnetic stirrer. The flask was evacuated and refilled with pure oxygen (balloon filled). Then the substrate (2.00 mmol) and isobutyraldehyde (IBA) (0.360 g, 5.00 mmol) was added into the solution with a syringe. The mixture was heated to reach the set temperature under O_2 atmosphere. The resulting mixture was vigorously stirred at 60.0°C under O_2 atmosphere for 7.00 h. The oxidation products were identified by comparison of their retention times with those of the authentic samples.

To test the reusability of the $\text{CXG}/[\text{V}^{\text{IV}}\text{O}(\text{HL})(\text{H}_2\text{O})(\text{CH}_3\text{OH})]$, after every usage, the catalyst was separated from reaction mixture by centrifuge, washed with CH_3CN and reused in the same reaction conditions again.

3. Results and discussion

3.1. Synthesis and characterization of H_3L and $[\text{V}^{\text{IV}}\text{O}(\text{HL})(\text{H}_2\text{O})(\text{CH}_3\text{OH})]$ complex

Fig. 3a shows the FT-IR spectra of the free H_3L ligand. There are no bands at 3,245 or 1,745 cm^{-1} , which would be expected for $\nu(\text{NH}_2)$ of the amino acid and $\nu(\text{C}=\text{O})$ of salicylaldehyde, respectively. Instead, a new prominent band at 1,612 cm^{-1} due to the azomethine $\nu(\text{C}=\text{N})$ linkage is observed. Comparison of the FT-IR spectra of free ligand and its vanadium complex, as shown in Fig. 3b, provides evidence for the coordination mode of the ligand. The infrared spectrum of complex displays an absorption band at 1,640 cm^{-1} which can be assigned to the $\text{C}=\text{N}$ stretching frequency of the coordinated ligand [29]. The shift of strong $\text{C}=\text{N}$ stretch in the FT-IR spectrum of complex indicates that the $\text{C}=\text{N}$ group

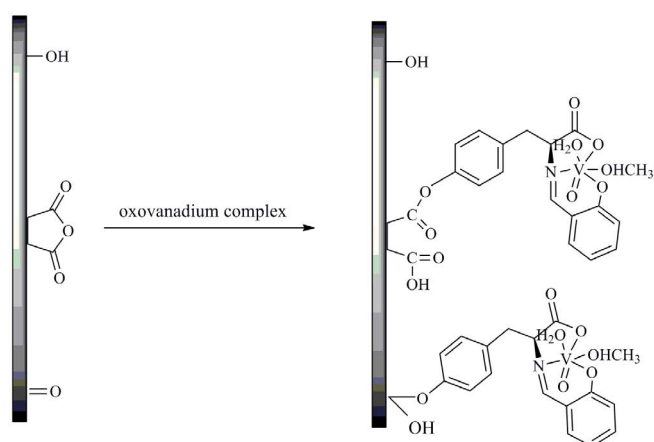


Fig. 2. Schematic presentation of the reactions that might occur between the hydroxyl groups of the metal complex and carbon xerogel surface groups for preparation of $\text{CXG}/[\text{V}^{\text{IV}}\text{O}(\text{HL})(\text{H}_2\text{O})(\text{CH}_3\text{OH})]$ [18,28].

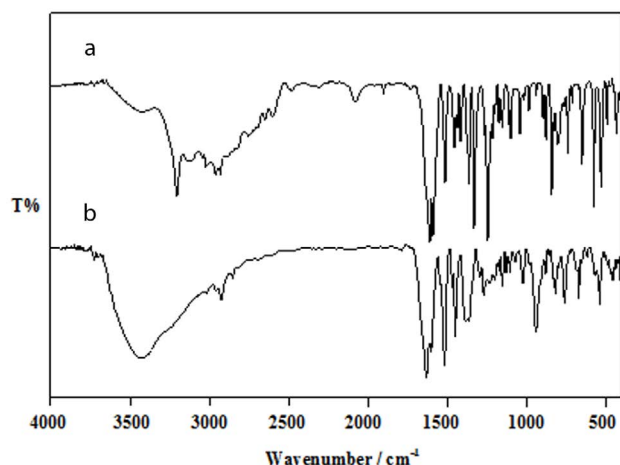


Fig. 3. FT-IR spectra of (a) H_3L and (b) $[VO(HL)(H_2O)(CH_3OH)]$.

of the Schiff base ligand is coordinated to the metal ion [30]. FT-IR spectrum of complex exhibits one sharp band at 948 cm^{-1} due to $\nu(V=O)$ mode [31]. In the spectrum of the complex, an extremely broad band at about $3,464\text{ cm}^{-1}$ is assigned to $-OH$, possibly involved in intermolecular hydrogen bonding.

Also, the oxidation state of vanadium has been proved by cyclic voltammeter (as shown in Fig. 4). The cyclic voltammogram of oxovanadium(IV) complex shows a well-defined red-ox process corresponding to the formation of the $V(IV)/V(V)$ couple at $E_{pa} = 0.35\text{ V}$ and the associated cathodic peak at $E_{pc} = 0.14\text{ V}$. This couple is quasi-reversible with $E_p = 0.21\text{ V}$ and the ratio of anodic to cathodic peak currents ($I_{pc}/I_{pa} \approx 1$) corresponding to a simple one electron process. The large separation between the cathodic and anodic peak (21 mV), indicates the quasi-reversible character [32,33].

The electronic spectra of the ligand and complex are also presented in Fig. 5. In the electronic spectra of the ligand, an absorption band in the 404 nm was observed, which may be associated with a $\pi \rightarrow \pi^*$ transition originating mainly in the azomethine chromophore (imine $\pi \rightarrow \pi^*$ transition). Bands at higher energies ($250\text{--}320\text{ nm}$) are attributed to the $\pi \rightarrow \pi^*$ transition of the benzene ring. In the electronic spectra of the complex, the azomethine chromophore $\pi \rightarrow \pi^*$ transition is shifted to ca. 370 nm indicating that the imino nitrogen is involved in coordination to the metal ion [34]. The shoulder at about 277 nm for complex corresponds to ligand metal charge transfer (LMCT) band of $V=O$ which it is seen at 274 nm for $[VO(acac)_2]$.

3.2. Synthesis and characterization of CXG and CXG/[VO(HL)(H₂O)(CH₃OH)]

The carbon xerogel material with immobilized $[VO(HL)(H_2O)(CH_3OH)]$ was characterized by FT-IR and AA to confirm the existence of oxovanadium complex onto the carbon xerogel surface. The surface oxygen groups on the activated carbon xerogel played an essential role in the immobilization of the $[VO(HL)(H_2O)(CH_3OH)]$. Hence, we can conclude that the metal complex is mainly immobilized through the reaction between the hydroxyl groups on the aldehyde

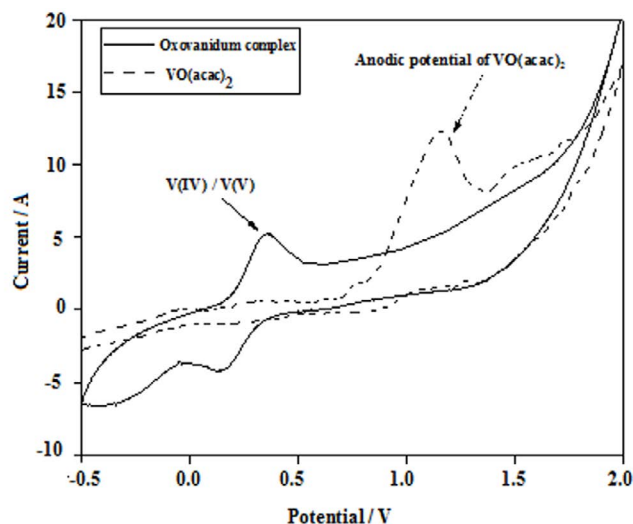


Fig. 4. Cyclic voltammograms of $[VO(HL)(H_2O)(CH_3OH)]$ and $VO(acac)_2$ in DMF containing 0.1 M tetrabutylammonium hexafluorophosphate (TBAH).

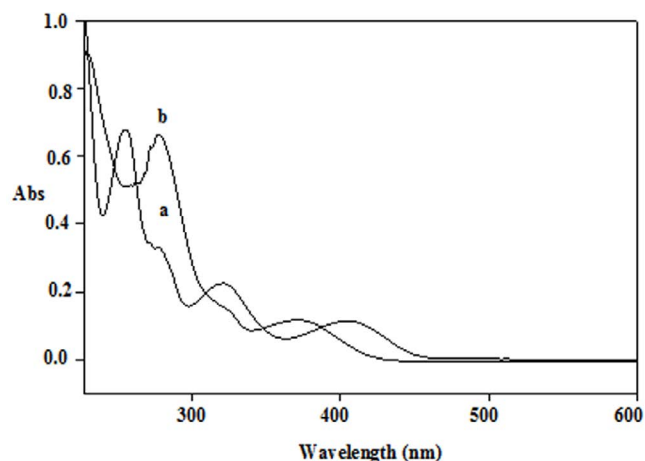


Fig. 5. UV-Vis spectra of (spectrum a) H_3L in the solution of methanol (10^{-5} M) and (spectrum b) $[VO(HL)(H_2O)(CH_3OH)]$ in the solution of methanol (10^{-5} M).

fragment of the H_3L ligand and some of the oxygen functional groups on the activated surface. We propose that immobilization of the functionalized oxovanadium complex onto the carbon xerogel surface should occur by the same anchoring mechanism, which involves the reaction between the surface carbonyl and carboxylic anhydride groups and the hydroxyl groups from the oxovanadium complex. By comparing these results with those of anchoring the same hydroxyl functionalized manganese complex onto oxidized activated carbons [18,28], we propose that immobilization of the functionalized oxovanadium complex onto carbon xerogel should occur by the same anchoring mechanism, which involves the reaction between the surface carbonyl and carboxylic anhydride groups and the hydroxyl groups from the oxovanadium complex. For the carbonyl groups, a direct nucleophilic attack of the hydroxyl can originate an

ether bond to the complex, and carboxylic anhydrides may also be subject to a nucleophilic attack from the hydroxyl groups, originating new carboxylic groups and an ester group, as depicted in Fig. 2.

The FT-IR spectra of the resorcinol–formaldehyde organogel (OG) and carbon xerogel (CXG) are illustrated in Fig. 6 and all the observed bands are in accordance with those reported in the literatures [35]. As shown in Fig. 6a, the stretching bands of C–H in the alkyl group appeared at 2,926 and 2,854 cm^{-1} , the band at 1,615 cm^{-1} shows C=C from aromatic ring. The absorption bands at 1,221 and 1,078 cm^{-1} are related to C–O–C stretching vibration of methylene ether bridges between two resorcinol molecules [35]. Fig. 6b shows the evolution of FT-IR spectrum after the pyrolysis. As the pyrolysis temperature increases from ambient to 800°C, most of the absorption peaks disappear. The –OH group's intensity is decreased and the other infrared active groups are completely eliminated at 800°C. When the pyrolysis temperature is raised to 800°C, only C–C vibration and FT-IR-active vibration can be found. It may be suggested that the graphitization process begins at below 800°C, while the sample is not still completely graphitized at 800°C, in accordance with the literature stating that graphitization temperatures of more than 2,000°C are typically necessary [36,37].

Fig. 7a shows the FT-IR spectrum of activated CXG by HNO_3 . The new peak in the FT-IR spectrum of activated carbogel at 1,728 cm^{-1} [38] is attributed to the carboxylic group, indicating that high densities of carboxylic group on carbogel surface have been generated. The band appearing at 1,590 cm^{-1} can be ascribed to the oxygen functional groups similar to a highly conjugated C=O stretching in carboxylic groups, and carboxylate moieties [39]. In addition, FT-IR spectrum of functionalized activated CXG by oxovanadium complex (Fig. 7b) shows bands at 1,251; 1,182; and 1,116 cm^{-1} associated with oxovanadium complex groups. In addition new band at 934 cm^{-1} can be assigned as

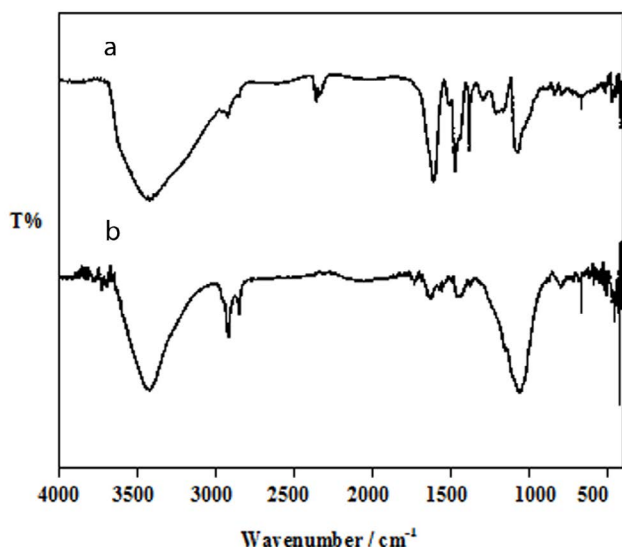


Fig. 6. FT-IR spectra of (spectrum a) resorcinol–formaldehyde organogel (OG) and (spectrum b) carbon xerogel after the pyrolysis at 800 °C (CXG).

V=O group. The other bands have been overlapped by similar bands of activated CXG at 1,500–1,700 cm^{-1} . Hence, the FT-IR characterization confirmed the successful anchoring of oxovanadium complex.

In addition, atomic absorption spectroscopy confirmed the presence of oxovanadium complex. The amount of vanadium ion within the CXG was determined by using AA after dissolution by HCl treatment and it was to be 8.5 $\mu\text{mol V/g CXG}$.

Textural characterization of the CXG and CXG/[$\text{V}^{\text{IV}}\text{O}(\text{HL})(\text{H}_2\text{O})(\text{CH}_3\text{OH})$] have been investigated using N_2 adsorption–desorption at -196°C . Fig. 8 shows the adsorption–desorption isotherms of the OG, CXG and CXG/[$\text{VO}(\text{HL})(\text{H}_2\text{O})(\text{CH}_3\text{OH})$]. It can be seen that the isotherms of the

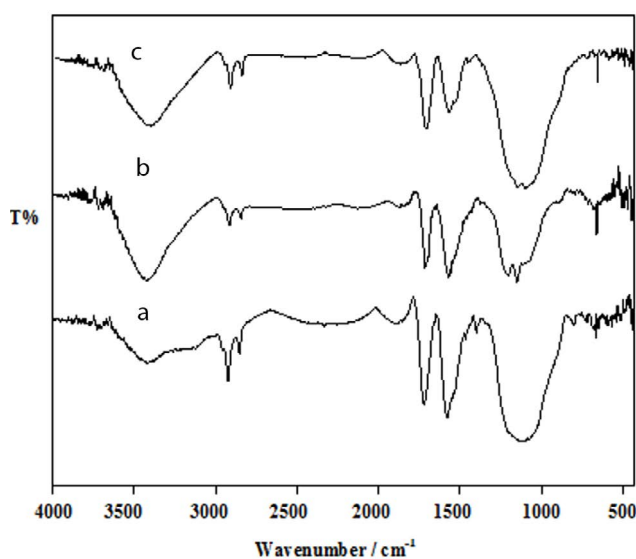


Fig. 7. FT-IR spectra of (spectrum a) activated carbon xerogel (CXG) by HNO_3 , (spectrum b) fresh CXG/[$\text{VO}(\text{HL})(\text{H}_2\text{O})(\text{CH}_3\text{OH})$] catalyst and (spectrum c) recycled CXG/[$\text{VO}(\text{HL})(\text{H}_2\text{O})(\text{CH}_3\text{OH})$] catalyst.

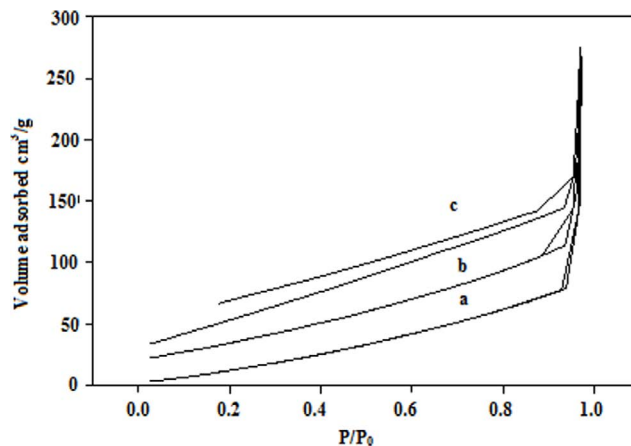


Fig. 8. Nitrogen adsorption and desorption isotherm at -196°C of (curve a) resorcinol–formaldehyde organogel (OG), (curve b) CXG/[$\text{VO}(\text{HL})(\text{H}_2\text{O})(\text{CH}_3\text{OH})$], and (curve c) carbon xerogel after the pyrolysis (CXG).

xerogels are of type IV/H3 (mesoporous) mixed to type I (microporous) isotherms, attributed to micro-mesoporous materials [40,41]. According to the isotherms of the samples, the specific surface area, specific pore volume, and pore size distribution of the samples were obtained and the results are shown in Table 1. The BET surface area of the samples decreased with $[V^{IV}O(HL)(H_2O)(CH_3OH)]$ loading, as depicted in Table 1, which was due to blocking of the pores by the complex [42,43]. Fig. 9 also illustrates, in the inset, the pore size distribution of the samples. It can be seen that the pores are distributed in the region of micropores and mesopores. In the micropore region all samples exhibit a common peak around 1.2 nm, indicating the presence of certain microporosity. On the other hand, all mesopores present a size below 5 nm.

In addition, the wide-angle XRD pattern demonstrated the organogel (Fig. 10a) to be graphitized after calcinations (Fig. 10b) and also activation by HNO_3 (Fig. 10c). For the sample before post treatment, a broad peak at around 19° is seen, indicative of amorphous materials. After pyrolysis at $800^\circ C$, two peaks at roughly 23° and 44° appear, which are the equivalents of the hexagonal graphite (002) ($2\theta = 26^\circ$) and (100) ($2\theta = 43^\circ$) reflections. The (002) diffraction peaks (ca. 26°) correspond to interlayer reflection [44]. The peak shift for the (002) reflection indicated an increase in the interlayer space. This shift might be attributed to the structure defects in the carbon materials [45,46].

Nano-particle size and morphology of CXG and CXG/ $[V^{IV}O(HL)(H_2O)(CH_3OH)]$ nano-particles have been characterized by SEM. The SEM images (Figs. 11a and b) show that the nano-networks of CXG and CXG/ $[V^{IV}O(HL)(H_2O)(CH_3OH)]$ have a similar morphology. Also CXG has about 45 nm and CXG/ $[V^{IV}O(HL)(H_2O)(CH_3OH)]$ has about 81 nm, Fig. 12.

3.3. Catalytic activity

The selective oxidation of olefins, especially employing oxygen as a terminal oxidant, has been believed one of the most important reactions in organic synthesis [47]. With the CXG/ $[V^{IV}O(HL)(H_2O)(CH_3OH)]$ catalyst in hand, we evaluated its catalytic activity for the aerobic oxidation of olefins.

Initially, 1-decene was selected as a model substrate, and the oxidation reaction was carried out in acetonitrile at $60.0^\circ C$ with CXG/ $[V^{IV}O(HL)(H_2O)(CH_3OH)]$ as catalyst, O_2 as oxidant and isobutyraldehyde as co-catalyst. In order to further optimize the process to achieve the maximum oxidation of 1-decene, the effect of different solvents was

studied. The conversion was highest for CH_3CN , being 35.0% after 7 h; CH_3CN was a better solvent medium than toluene (8.00%), ethyl acetate (10.0%) and *n*-hexane (0%). The difference is explained by the high solubility of reagents in CH_3CN .

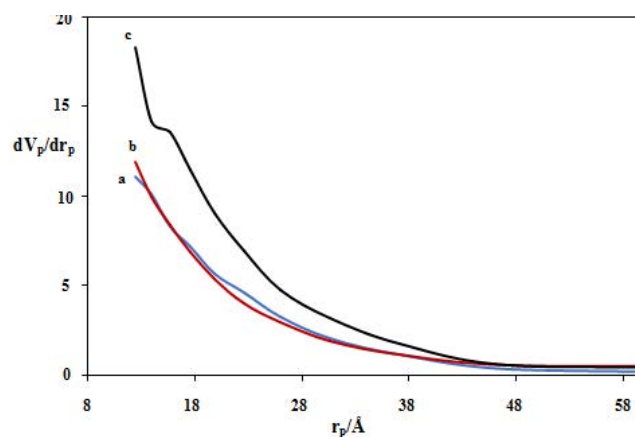


Fig. 9. Pore size distribution of (curve a) resorcinol–formaldehyde organogel (OG), (curve b) CXG/ $[V^{IV}O(HL)(H_2O)(CH_3OH)]$, and (curve c) carbon xerogel after the pyrolysis (CXG).

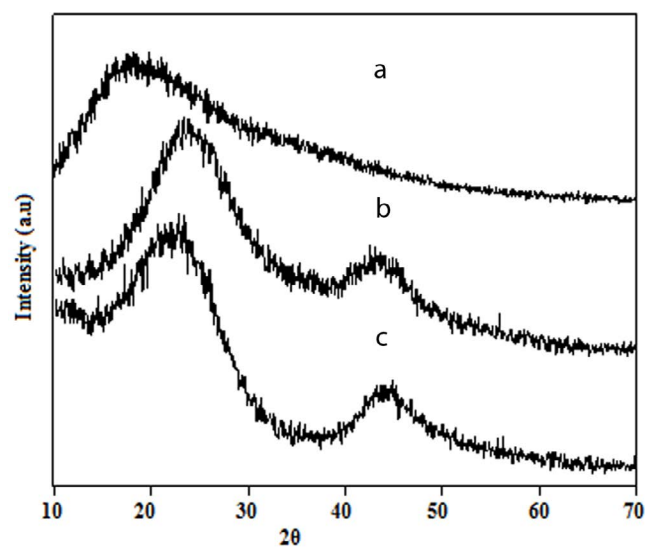


Fig. 10. XRD pattern of (curve a) resorcinol–formaldehyde organogel (OG), (curve b) CXG pyrolyzed at $800^\circ C$, and (curve c) activated CXG by HNO_3 .

Table 1
Surface area and textural characteristics of samples

Sample	Specific surface area ($m^2 g^{-1}$)	Pore volume ($cm^3 g^{-1}$) ^a	Pore diameter (nm)	Pore volume micropores ($cm^3 g^{-1}$) ^b	Pore volume mesopores ($cm^3 g^{-1}$) ^b
RF OG	51.14	1.14	2.72	0.376	0.756
CXG	116.53	0.852	2.428	0.529	0.323
CXG/ $[V^{IV}O(HL)(H_2O)(CH_3OH)]$	80.995	0.966	2.231	0.460	0.506

^a S_{BET} calculated with the Brunauer–Emmett–Teller (BET) equation.

^bMicropore volumes (V_{Mic} volume of pores of width lower than 2 nm) determined with the MP plot (*t*-curve).

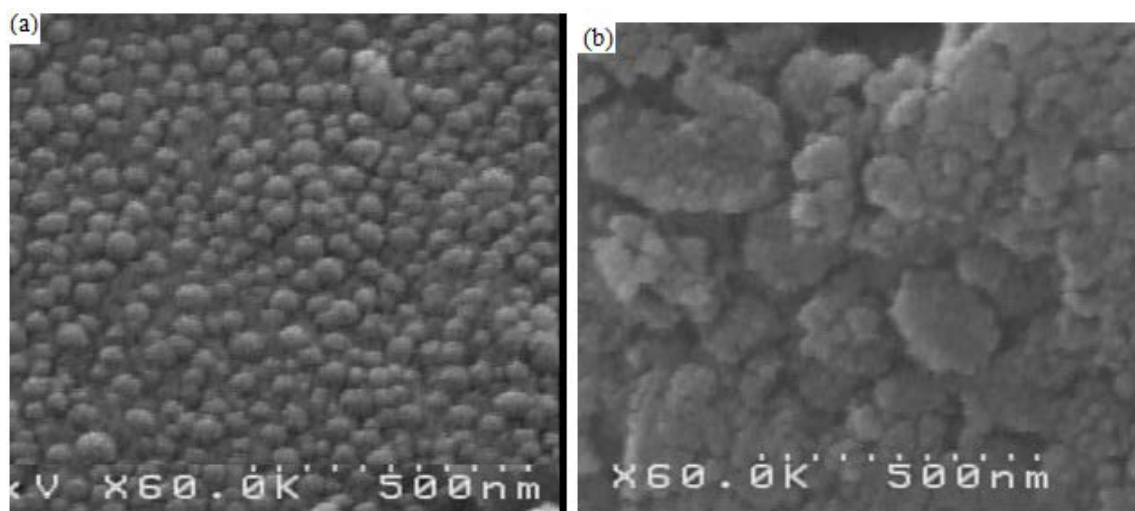


Fig. 11. SEM images of (a) carbon xerogel after the pyrolysis (CXG) and (b) CXG/[VO(HL)(H₂O)(CH₃OH)].

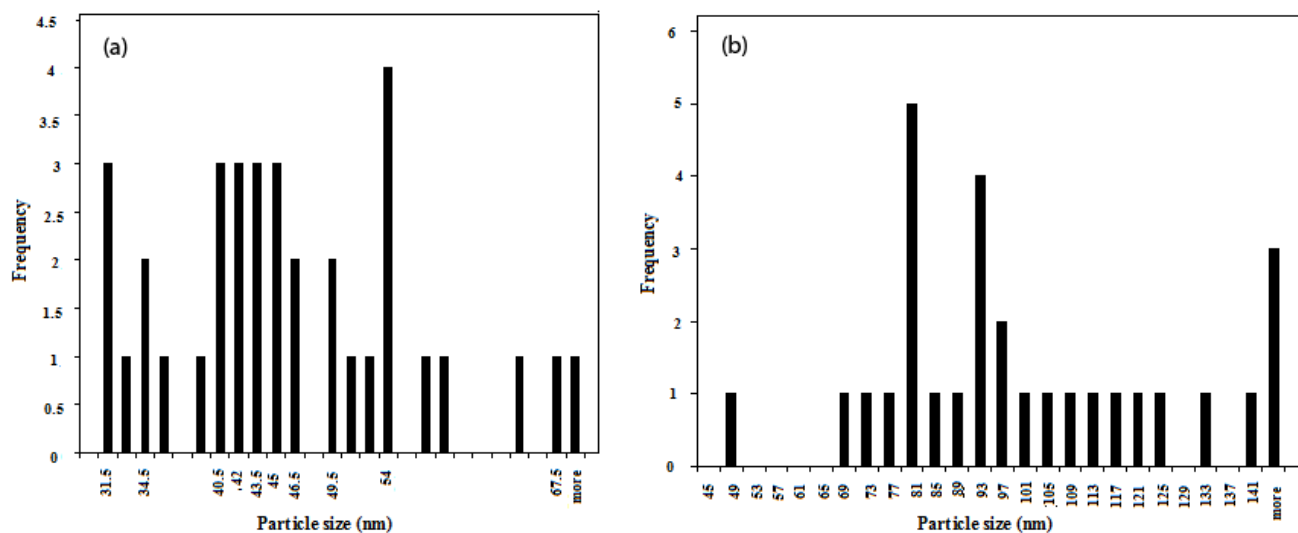


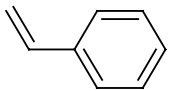
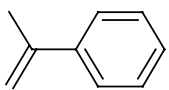
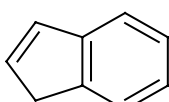
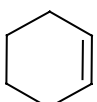
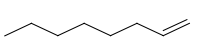
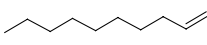
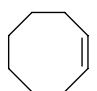
Fig. 12. Particle size distribution histogram of (a) carbon xerogel after the pyrolysis (CXG) and (b) CXG/[VO(HL)(H₂O)(CH₃OH)] nanoparticles (detection of particles' average size of about 45 nm).

Alternatively, the reaction was carried out at different temperatures. When the temperature was increased (from 25.0°C to 60.0°C), the conversion increased correspondingly (from 0% to 35.0%). Increasing temperature to 80°C did not improve the conversion.

To establish the scope for the activity of CXG/[VO(HL)(H₂O)(CH₃OH)], this study was further extended to the catalytic oxidation of several linear and cyclic olefins, namely α -methylstyrene, cis-cyclooctene, 1-octene, styrene, cyclohexene (Table 2). Generally, the present catalytic system was completely selective for the epoxidation of cyclooctene, indene, 1-octene, 1-decene and styrene, while for α -methyl styrene, acetophenone was the byproduct. The catalytic activity of α -methyl styrene is higher than styrene. It should be noted that electronic effects due to the methyl substituent were important, then, α -methyl styrene as a more electron-rich olefin would show higher activity relative to the styrene.

As can be seen in Table 2, the order of increasing reactivities based on either conversions or turn over numbers (TONs) are as cis-cyclooctene > cyclohexene > 1-octene > 1-decene. To explain this trend, two determining parameters of electronic and steric effects should be taken into consideration. The higher electronic density of the double bond is expected to show more epoxidation reactivity. Therefore, cyclooctene and cyclohexene with double bonds driven from secondary carbons should exhibit more activities in comparison with 1-octene and 1-decene which contain double bonds between secondary and primary carbons. On the other hand, cyclooctene is more reactive than cyclohexene due to the presence of more electrons donating (CH₂)₆ cyclic bridges connected to the double bond. Furthermore, 1-decene is epoxidized slower than 1-octene since larger octyl group connected to double bond sterically hinders it in approaching the catalyst metal center with respect to 1-octene which its double bond carrying a smaller hexyl group [48].

Table 2
Aerobic oxidation of alkenes catalyzed by CXG/[VO(HL)(H₂O)(CH₃OH)]^a

Entry	Substrate	Conversion (%) ^b	Epoxide selectivity (%)
1		67.5	85.0
2		90.0	>99.0
3		8.50	>99.0
4		68.0	>99.0
5		50.0	>99.0
6		35.0	>99.0
7		96.0	>99.0

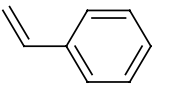
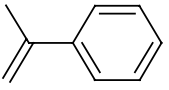
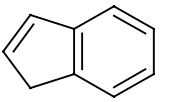
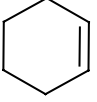
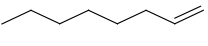
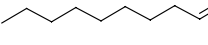
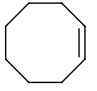
^aReaction conditions: catalyst (0.0850 μmol of V(IV)), substrate (2.00 mmol), CH₃CN (5.00 mL), IBA (5.00 mmol), O₂ as an oxidant and temperature 60.0°C; time 7.00 h.

^bConversions are based on the starting substrates.

Epoxide selectivity and conversion of CXG/[VO(HL)(H₂O)(CH₃OH)] in the oxidation of styrene is higher than the previously reported systems such as VO-GO and VO-salen-GO [49], PS-[VO(ligand)_n] [50], VO-salen-SBA [51], and MRGO/Fe₃O₄@C-salen-V [52]. This behavior could be related to the surface chemistry of the carbon material plays a decisive role on its catalytic properties, providing active sites capable of chemisorbing the reactants and forming surface intermediates of adequate strength. In addition to the green nature of the present catalytic system (O₂), mild conditions such as low temperature in comparison other reported systems and lower catalyst amount, the recyclability and simplicity of CXG/[VO(HL)(H₂O)(CH₃OH)] catalyst are favored over those of the reported catalysts.

In continuous, the performance of the homogeneous catalyst, [VO(HL)(H₂O)(CH₃OH)], was also studied by running the oxidation of olefins under the optimized reaction conditions, after 7.00 h (Table 3). The homogeneous catalyst, [VO(HL)(H₂O)(CH₃OH)], was less active with similar selectivity for the oxidation of olefins in comparison with heterogeneous catalyst (Table 3, Entries 1–7). In fact, the activity and selectivity of the anchored complex can even be enhanced with respect to the homogeneous systems. This may result from a confinement effect, that is, as a result of site isolation, that is, the anchored complexes are prevented from reacting with each other, as they could do in homogeneous medium, leading to the formation of inactive

Table 3
Aerobic oxidation of alkenes catalyzed by [VO(HL)(H₂O)(CH₃OH)]^a

Entry	Substrate	Conversion (%) ^b	Epoxide selectivity (%)
1		45.0	80.0
2		67.0	>99.0
3		0	>99.0
4		40.0	>99.0
5		21.0	>99.0
6		13.0	>99.0
7		78.0	>99.0

^aReaction conditions: catalyst (0.0850 μmol of V(IV)), substrate (2.00 mmol), CH₃CN (5.00 mL), IBA (5.00 mmol), O₂ as an oxidant and temperature 60.0°C; time 7.00 h.

^bConversions are based on the starting substrates.

dimeric species [29]. As a result, the anchored complexes were found to be very stable and reusable catalysts for the epoxidation of olefins. The surface chemistry of the carbon material plays a decisive role on its catalytic properties, providing active sites capable of chemisorbing the reactants and forming surface intermediates of adequate strength. In fact, introduction of transition metal complexes onto the surface of porous carbons can increase the efficiency of catalysts. Similar results have been reported in some literatures [53,54].

3.4. Catalyst recycling

The recyclability of CXG/[VO(HL)(H₂O)(CH₃OH)] was investigated in several runs of the oxidation reaction of 1-decene. At the end of the reaction, the catalyst was separated by centrifuge and its activity in the next runs was investigated. The catalytic activity of CXG/[VO(HL)(H₂O)(CH₃OH)] is preserved even after five runs and yield of the reaction does not change significantly, as shown in Table 4.

Atomic adsorption spectroscopy of reaction mixture after catalyst separation also confirmed that no free vanadium ions are present in the solution. These findings confirmed the absence of catalyst leaching. The stability of the supported catalyst was also investigated. In these experiments, the catalyst was separated from the reaction mixture after each experiment, washed, dried and characterized by FT-IR as shown in Fig. 7c.

Table 4
Effect of catalyst recycling on the oxidation of 1-decene^a

Number of cycle	Conversion ^b (%)	Epoxide selectivity (%)
Fresh	35.0	>99.0
1	33.0	>99.0
2	35.0	>99.0
3	34.0	>99.0
4	35.0	>99.0
5	34.0	>99.0

^aReaction conditions: catalyst, (0.0850 μmol), substrate (2.00 mmol), IBA (5.00 mmol), CH₃CN (5.00 mL), O₂ as an oxidant and temperature 60.0°C; time 7.00 h.

^bConversions are based on the starting substrates.

4. Conclusions

Herein porous carbon was used as support for anchoring oxovanadium complex with catalytic activity, for the preparation of supported metal catalyst. CXG/[VO(HL)(H₂O)(CH₃OH)] was found to be highly efficient catalyst for epoxidation of olefins with O₂ as the oxidant. In summary, we have developed an efficient system with high activity for the aerobic epoxidation of olefins by using CXG/[VO(HL)(H₂O)(CH₃OH)] under mild reaction conditions. The catalyst was stable and could be easily recycled. Various aromatic and aliphatic epoxides were produced from the corresponding olefins with excellent selectivity, and high yields. Synergic effect of the CXG and catalyst plays critical role in enhancing the catalytic activity of CXG/[VO(HL)(H₂O)(CH₃OH)]. Easy tuning of porous carbon surface chemistry through chemical and thermal post-treatments and subsequent functionalization achieved. Carboxylic acids and anhydrides, phenol and carbonyl surface groups used to anchor oxovanadium complexes, directly. The strategy used, covalent bonding of the complex onto the carbon surface prevents leaching, leading to stable and reusable catalysts. The catalyst was recovered easily and reused for five runs without significant loss of activity.

Acknowledgments

The authors are thankful to University of Zanjan for financial support of this study.

References

- [1] M. Pérez-Cadenas, C. Moreno-Castilla, F. Carrasco-Marín, A.F. Pérez-Cadenas, Surface chemistry, porous texture, and morphology of N-doped carbon xerogels, *Langmuir*, 25 (2009) 466–470.
- [2] A.H. Moreno, A. Arenillas, E.G. Calvo, J.M. Bermúdez, J.A. Menéndez, Carbonisation of resorcinol–formaldehyde organic xerogels: effect of temperature, particle size and heating rate on the porosity of carbon xerogels, *J. Anal. Appl. Pyrolysis*, 100 (2013) 111–116.
- [3] E.G. Calvo, J.A. Menéndez, A. Arenillas, Designing Nano-structured Carbon Xerogels, Chapter 9, P.M. Rahman Ed., *Nanomaterials*, In Tech, Rijeka, 2011, pp. 87–234.
- [4] R.W. Pekala, J.C. Farmer, C.T. Alviso, T.D. Tran, S.T. Mayer, J.M. Miller, B. Dunn, Carbon aerogels for electrochemical applications, *J. Non-Cryst. Solids*, 225 (1998) 74–80.
- [5] R. Saliger, U. Fischer, C. Herta, J. Fricke, High surface area carbon aerogels for supercapacitors, *J. Non-Cryst. Solids*, 225 (1998) 81–85.
- [6] E. Frackowiak, F. Béguin, Carbon materials for the electrochemical storage of energy in capacitors, *Carbon*, 39 (2001) 937–950.
- [7] K.Y. Kang, B.I. Lee, J.S. Lee, Hydrogen adsorption on nitrogen-doped carbon xerogels, *Carbon*, 47 (2009) 1171–1180.
- [8] T. Yamamoto, T. Sugimoto, T. Suzuki, S.R. Mukai, H. Tamon, Preparation and characterization of carbon cryogel microspheres, *Carbon*, 40 (2002) 1345–1351.
- [9] L. Zubizarreta, J.A. Menéndez, N. Job, J.P. Marco-Lozar, J.P. Pirard, J.J. Pis, A. Linares-Solano, D. Cazorla-Amorós, A. Arenillas, Ni-doped carbon xerogels for H₂ storage, *Carbon*, 48 (2010) 2722–2733.
- [10] N. Job, B. Heinrichs, F. Ferauche, F. Noville, J. Marien, J.-P. Pirard, Hydrodechlorination of 1,2-dichloroethane on Pd–Ag catalysts supported on tailored texture carbon xerogels, *Catal. Today*, 102–103 (2005) 234–241.
- [11] N. Job, B. Heinrichs, S. Lambert, J.-P. Pirard, J.-F. Colomer, B. Vertruyen, J. Marien, Carbon xerogels as catalyst supports: study of mass transfer, *AIChE J.*, 52 (2006) 2663–2676.
- [12] N. Job, M.F. Ribeiro Pereira, S. Lambert, A. Cabiac, G. Delahay, J.-F. Colomer, J. Marien, J.L. Figueiredo, J.-P. Pirard, Highly dispersed platinum catalysts prepared by impregnation of texture-tailored carbon xerogels, *J. Catal.*, 240 (2006) 160–171.
- [13] N. Job, J. Marie, S. Lambert, S. Berthon-Fabry, P. Achar, Carbon xerogels as catalyst supports for PEM fuel cell cathode, *Energy Convers. Manage.*, 49 (2008) 2461–2470.
- [14] A.M.T. Silva, B.F. Machado, J.L. Figueiredo, J.L. Faria, Controlling the surface chemistry of carbon xerogels using HNO₃-hydrothermal oxidation, *Carbon*, 47 (2009) 1670–1679.
- [15] N. Mahata, M.F.R. Pereira, F. Suárez-García, A. Martínez-Alonso, J.M.D. Tascón, J.L. Figueiredo, Tuning of texture and surface chemistry of carbon xerogels, *J. Colloid Interface Sci.*, 324 (2008) 150–155.
- [16] A.R. Silva, M. Martins, M.M.A. Freitas, A. Valente, C. Freire, B. de Castro, J.L. Figueiredo, Immobilisation of amine-functionalised nickel(II) Schiff base complexes onto activated carbon treated with thionyl chloride, *Microporous Mesoporous Mater.*, 55 (2002) 275–284.
- [17] M.C. Román-Martínez, J.A. Díaz-Auñón, C. Salinas-Martínez de Lecea, H. Alper, Rhodium-diphosphine complex bound to activated carbon: An effective catalyst for the hydroformylation of 1-octene, *J. Mol. Catal. A: Chem.*, 213 (2004) 177–182.
- [18] N. Mahata, A.R. Silva, M.F. Pereira, C. Freire, B. de Castro, J.L. Figueiredo, Anchoring of a [Mn(salen)Cl] complex onto mesoporous carbon xerogels, *J. Colloid Interface Sci.*, 311 (2007) 152–158.
- [19] A.R. Silva, J. Vital, J.L. Figueiredo, C. Freire, B. de Castro, Activated carbons with immobilized Mn(III) salen complexes as heterogeneous catalysts in the epoxidation of olefins: influences of support and ligand functionalization on selectivity and reusability, *New J. Chem.*, 27 (2003) 1511–1517.
- [20] A.R. Silva, J.L. Figueiredo, C. Freire, B. de Castro, Manganese(III) salen complexes anchored onto activated carbon as heterogeneous catalysts for the epoxidation of olefins, *Microporous Mesoporous Mater.*, 68 (2004) 83–89.
- [21] M. Sutradhar, L.M.D.R.S. Martins, S.A.C. Carabineiro, M.F.C. Guedes da Silva, J.G. Buijnsters, J.L. Figueiredo, A.J.L. Pombeiro, Oxidovanadium(V) complexes anchored on carbon materials as catalysts for the oxidation of 1-phenylethanol, *Chem. Cat. Chem.*, 8 (2016) 2254–2266.
- [22] A.R. Silva, M.M.A. Freitas, C. Freire, B. de Castro, J.L. Figueiredo, Heterogenization of a functionalized Copper(II) Schiff base complex by direct immobilization onto an oxidized activated carbon, *Langmuir*, 18 (2002) 8017–8024.
- [23] F. Maia, N. Mahata, B. Jarrais, A.R. Silva, M.F.R. Pereira, C. Freire, J.L. Figueiredo, Jacobsen catalyst anchored onto modified carbon xerogel as enantioselective heterogeneous catalyst for alkene epoxidation, *J. Mol. Catal. A: Chem.*, 305 (2009) 135–141.

- [24] D. Heinert, A.E. Martell, Pyridoxine and pyridoxal analogs. V. Syntheses and infrared spectra of Schiff bases, *J. Am. Chem. Soc.*, 84 (1962) 3257–3263.
- [25] M. Ghorbanloo, M. Jaworska, P. Paluch, G.-D. Li, L.-J. Zhou, Synthesis, characterization, and catalytic activity for thioanisole oxidation of homogeneous and heterogeneous binuclear manganese(II) complexes with amino acid-based ligands, *Transition Met. Chem.*, 38 (2013) 511–521.
- [26] L. Zubizarreta, A. Arenillas, A. Domínguez, J.A. Menéndez, J.J. Pis, Development of microporous carbon xerogels by controlling synthesis conditions, *J. Non-Cryst. Solids*, 354 (2008) 817–825.
- [27] J.L. Figueiredo, M.F.R. Pereira, M.M.A. Freitas, J.J.M. Orfao, Modification of the surface chemistry of activated carbons, *Carbon*, 37 (1999) 1379–1389.
- [28] J.L. Figueiredo, Functionalization of porous carbons for catalytic applications, *J. Mater. Chem. A*, 1 (2013) 9351–9364.
- [29] M. Ghorbanloo, A. Mohamadi, M. Amini, J. Tao, Use of a molybdenum(VI) dioxide complex as a homogeneous and heterogeneous magnetically recoverable epoxidation catalyst, *Transition Met. Chem.*, 40 (2015) 321–331.
- [30] R. Bikas, V. Lippolis, N. Noshiranzadeh, H. Farzaneh-Bonab, A.J. Blake, M. Siczek, H. Hosseini-Monfared, T. Lis, Electronic effects of aromatic rings on the Catalytic activity of dioxidomolybdenum(VI)-hydrazone complexes, *Eur. J. Inorg. Chem.*, 6 (2017) 999–1006.
- [31] M. Ghorbanloo, S. Jafari, R. Bikas, M.S. Krawczyk, T. Lis, Dioxidovanadium(V) complexes containing thiazol-hydrazone NNN-donor ligands and their catalytic activity in the oxidation of olefins, *Inorg. Chim. Acta*, 557 (2017) 15–24.
- [32] M. Kalanithi, D. Kodimunthiri, M. Rajarajanb, P. Tharmaraj, Synthesis, characterization and biological activity of some new VO(IV), Co(II), Ni(II), Cu(II) and Zn(II) complexes of chromone based NNO Schiff base derived from 2-aminothiazole, *Spectrochim. Acta, Part A*, 82 (2011) 290–298.
- [33] J.C. Dutton, G.D. Fallon, K.S. Murray, Synthesis, structure, ESR spectra, and redox properties of (N,N'-ethylenebis(thio salicylideneaminato))oxovanadium(IV) and of related {S,N} chelates of vanadium(IV), *Inorg. Chem.*, 27 (1988) 34–38.
- [34] O.E. Offiong, E. Nfor, A.A. Ayi, S. Martelli, Synthesis, spectral and cytotoxicity studies of palladium(II) and platinum(II) amino acid Schiff base complexes, *Transition Met. Chem.*, 25 (2000) 369–373.
- [35] R.W. Pekala, Organic aerogels from the polycondensation of resorcinol with formaldehyde, *J. Mater. Sci.*, 24 (1989) 3221–3227.
- [36] A. Oberlin, Carbonization and graphitization, *Carbon*, 22 (1984) 521–541.
- [37] W.-C. Li, A.-H. Lu, S.-C. Guo, Characterization of the microstructures of organic and carbon aerogels based upon mixed cresol-formaldehyde, *Carbon*, 39 (2001) 1989–1994.
- [38] J.-W. Shim, S.-J. Park; S.-K. Ryu, Effect of modification with HNO₃ and NaOH on metal adsorption by pitch-based activated carbon fibers, *Carbon*, 39 (2001) 1635–1642.
- [39] Y.F. Jia, K.M. Thomas, Adsorption of cadmium ions on oxygen surface sites in activated carbon, *Langmuir*, 16 (2000) 1114–1121.
- [40] N. Brun, S.A. Wohlgemuth, P. Osiceanu, M.M. Titirici, Original design of nitrogen-doped carbon aerogels from sustainable precursors: application as metal-free oxygen reduction catalysts, *Green Chem.*, 15 (2013) 2514–2524.
- [41] J.Y. Ying, C.P. Mehnert, M.S. Wong, Synthesis and applications of supramolecular-templated mesoporous materials, *Angew. Chem. Int. ed.*, 38 (2004) 56–77.
- [42] C. Moreno-Castilla, F.J. Maldonado-Hódar, Carbon aerogels for catalysis applications: an overview, *Carbon*, 43 (2005) 455–465.
- [43] O. Czakkel, E. Geissler, I.M. Szilágyi, E. Székely, K. László, Cu-doped resorcinol-formaldehyde (RF) polymer and carbon aerogels, *J. Colloid Interface Sci.*, 337 (2009) 513–522.
- [44] L. Zhao, N. Baccile, S. Gross, Y.J. Zhang, W. Wei, Y.H. Sun, M. Antonietti, M.-M. Titirici, Sustainable nitrogen-doped carbonaceous materials from biomass derivatives, *Carbon*, 48 (2010) 3778–3787.
- [45] L. Yu, C. Falco, J. Weber, R.J. White, J.Y. Howe, M.-M. Titirici, Carbohydrate-derived hydrothermal carbons: a thorough characterization study, *Langmuir*, 28 (2012) 12373–12383.
- [46] S.-A. Wohlgemuth, F. Vilela, M.-M. Titirici, M. Antonietti, A one-pot hydrothermal synthesis of tunable dual heteroatom-doped carbon microspheres, *Green Chem.*, 14 (2012) 741–749.
- [47] X. He, L. Chen, X. Zhou, H. Ji, Recyclable Pd supported catalysts with low loading for efficient epoxidation of olefins at ambient conditions, *Catal. Commun.*, 83 (2016) 78–81.
- [48] M. Ghorbanloo, R. Bikas, G. Małecki, New molybdenum(VI) complexes with thiazole-hydrazone ligand: preparation, structural characterization, and catalytic applications in olefin epoxidation, *Inorg. Chim. Acta*, 445 (2016) 8–16.
- [49] H. Su, S. Wu, Z. Li, Q. Huo, J. Guan, Q. Kan, Co(II), Fe(III) or VO(II) Schiff base metal complexes immobilized on graphene oxide for styrene epoxidation, *Appl. Organomet. Chem.*, 29 (2015) 462–467.
- [50] M.R. Maurya, A. Arya, P. Adão, J.C. Pessoa, Immobilisation of oxovanadium(IV), dioxomolybdenum(VI) and copper(II) complexes on polymers for the oxidation of styrene, cyclohexene and ethylbenzene, *Appl. Catal., A*, 351 (2008) 239–252.
- [51] Y. Yang, Y. Zhang, S. Hao, J. Guan, H. Ding, F. Shang, P. Qiu, Q. Kan, Heterogenization of functionalized Cu(II) and VO(IV) Schiff base complexes by direct immobilization onto amino-modified SBA-15: styrene oxidation catalysts with enhanced reactivity, *Appl. Catal., A*, 381 (2010) 274–281.
- [52] Z. Li, S. Wu, D. Zheng, H. Ding, X. Wang, X. Yang, Q. Huo, J. Guan, Q. Kan, Enhanced aerobic epoxidation of styrene with copper(II), cobalt(II), iron(III), or oxovanadium(IV) salen complexes immobilized onto carbon-coated Fe₃O₄ nanoparticles hybridized with graphene sheets, *Chem. Plus Chem.*, 79 (2014) 716–724.
- [53] C. Alegre, E. Baquedano, M.E. Gálvez, R. Moliner, M.J. Lázaro, Tailoring carbon xerogels' properties to enhance catalytic activity of Pt catalysts towards methanol oxidation, *Int. J. Hydrogen Energy*, 40 (2015) 14736–14745.
- [54] C. Arbizzani, S. Beninati, E. Manferrari, F. Soavi, M. Mastragostino, Cryo- and xerogel carbon supported PtRu for DMFC anodes, *J. Power Sources*, 172 (2007) 578–86.